Insights into Formation and Relaxation of Shear-Induced Nucleation Precursors in Isotactic Polystyrene

Fiorenza Azzurri and Giovanni C. Alfonso*

Department of Chemistry and Industrial Chemistry, University of Genova, Via Dodecaneso 31, 16146 Genova, Italy

Received July 3, 2007; Revised Manuscript Received November 30, 2007

ABSTRACT: Rheooptical experiments on narrow isotactic polystyrene (*i*-PS) fractions have been carried out to investigate temperature and molar mass dependence of the lifetime of shear-induced nucleation precursors. Similar to *i*-poly(1-butene) and *i*-polypropylene, the survival of the flow-induced structures lasts very long, even at temperatures well above the measured melting point of the crystals. It has been observed that the decrease of concentration of nucleation precursors follows a first-order kinetics with a strongly temperature-dependent rate constant. The apparent activation energy of the overall relaxation process is around 400 kJ/mol, of the same order of magnitude previously found for other semicrystalline polymers. A comparative analysis of the apparent activation energy data for different polymers, coupled with morphological evidence, suggests that the rate-determining step in the evolution of the system toward the equilibrium state in the melt is the detachment of stems from the lateral surface of flow-induced oriented bundles, present either as isolated entities, in the case of pointlike nuclei, or as rows alternated by disordered nanodomains, in the long threads of the shish. Thanks to the monodisperse character of the investigated samples, the molar mass dependence of lifetime of oriented nucleation precursors has also been established.

Introduction

Many experimental evidences acquired in the past decades have clearly established that shear flow strongly affects polymer crystallization, from both kinetic and morphological points of view.[1−12] Molecular characteristics, such as chain branching[13−15] and composition,[13,15−17] and imposed flow conditions, such as temperature[18−23] and shear rate,[20,22−25] are variables that dictate the development of flow-induced structures and have strong impact on all facets of the crystallization process. Through ingenious laboratory scale experiments, it has been found that the lower is the temperature and the higher is the applied shear rate, the greater the effect on solidification is. The relevant role of weight-average molar mass was also studied, and clear evidence that the effect of flow fields on crystallization is enhanced in high molar mass polymers was gained.[5,18,21,26−33] Experiments performed on polydispersed samples demonstrated that the presence of small amounts of high molecular weight chains are sufficient to drastically affect the crystallization kinetics of sheared polymers, thus suggesting that the entangled long molecules are mainly responsible for the formation of nucleation precursors under shear.[27,31,32] Since long chains have a greater chance of being involved in a number of nucleation precursors, they require long time to disengage and to relax after having being perturbed by the applied flow field, thus playing a major role in determining the stability of flow-induced oriented structures. In this context, the extensive early investigations carried out by Janeschitz-Kriegl and collaborators in Linz must be highlighted. They were the first to understand that a competition exists between formation of nucleation precursors and relaxation processes in shear-induced crystallization.[34]

From a microscopic point of view, in-situ and ex-situ experiments have shown that shear flow promotes local chain alignment and generates nanodomains with an intermediate degree of order, usually referred to as crystal nucleation precursors,[4−7,21,35−44] which exhibit a very long lifetime, even at temperatures above the nominal melting temperature of the investigated polymer.[22,37−39] By means of in-situ SAXS−WAXD experiments, some insight into the structural organization of flow-induced precursors was recently acquired. Somani et al.[37,38] found that development of crystalline order proceeds through the formation of a stable shish structure, containing a linear assembly of primary nuclei, on which folded chain lamellae, kebabs, subsequently grow through an epitaxial secondary nucleation process. The same picture was also deduced from the spatially resolved X-ray micro-SAXS/WAXD investigation we carried out on unfractionated isotactic polystyrene sheared by the fiber pulling method.[39] It was found that shearing isotactic polystyrene at 260 °C leads to formation of quasi-ordered clusters whose geometrical characteristics, size, and orientation distribution strongly depend on the distance from the fiber surface and, therefore, on the intensity of the flow field.[45] According to a recent paper by Kanaya et al.,[43] birefringent oriented structures, with length in the micrometer range, form whenever a pulse shear is imposed on isotactic polystyrene at temperatures as high as 250 °C.

Once formed, these shear-induced structures exhibit very long lifetimes if held in quiescent conditions, even at temperatures above the nominal melting temperature of spherulites.[21,37−39,46−48] According to Janeschitz-Kriegl, the small cross section characterizing bundles of chain segments implies a lower end surface free energy, thus increasing their thermal stability in comparison to folded chain crystals; therefore, threadlike nuclei formed at high deformation rates in a temperature range close to the equilibrium melting point are practically stable, even at temperatures higher than the melting point of spherulites.[47,48]

Our previous experiments on poly(ethylene oxide), polypropylene,[18] and isotactic poly(1-butene)[21] have unambiguously shown that the relaxation process associated with the decay of concentration of shear-induced nucleation precursors strongly depends on temperature and molecular weight. In light of these experimental evidences, a complex mechanism of destructuring

* Corresponding author. E-mail: alfonso@chimica.unige.it.

10.1021/ma071475e CCC: $40.75
Published on Web 01/15/2008

Table 1. Molecular Characteristics of the i-PS Samples

sample code	$\bar{M}_n$ (kg/mol)	$\bar{M}_w$ (kg/mol)	$\bar{M}_w/\bar{M}_n$	isotacticity index, %
W		939[a]	6.4	97
F1	234	291	1.24	96 ± 2
F2	563	605	1.07	96 ± 2
F3	989	1022	1.03	96 ± 2
F4	1540	1700	1.10	96 ± 2

[a] Viscosity average molar mass, M_η.

of clusters and randomization of chain segments was theorized.[49] For what concerns the effect of chain length on the overall relaxation kinetics, experiments performed with polydispersed samples indicated that the lifetime scales with molecular weight according to a power law with exponent about 3.[21] However, it is known that the high molecular weight tail of the distribution dictates the crystallization in sheared systems.[26,29−32] Therefore, because of the wide molecular wide distribution of the previously used samples, the precise role of molecular dimensions on the lifetime of nucleation precursors still needs to be addressed with better accuracy.

The role of chain length and temperature on the relaxation of shear- induced nucleation precursors in four narrow fractions of isotactic polystyrene will be illustrated, and the results will be discussed in terms of memory effects on polymer crystallization.

Experimental Section

Materials and Techniques. The polymers used to investigate the role of temperature and chain length on lifetime of shear-induced nucleation precursors were four very sharp fractions of isotactic polystyrene (*i*-PS), kindly provided by Prof. H. Marand, Virginia Tech University. As reported in Table 1, the *i*-PS fractions exhibit the same isotacticity index and cover a range of about 1 order of magnitude in molecular weight, from ca. 300 000 to above 1.5 million. Because of the very small amount of available materials, of the order of 20 mg each fraction, experiments on fractions were preceded by a preliminary investigation on an unfractioned sample with similar isotacticity index which was purchased from Polymer Laboratories, Ltd., UK.

Films, about 150 μm thick, were obtained from the as-received powder by compression molding in a Carver press at a temperature of 300 °C for 3 min, followed by quenching in cold water. To prepare samples for the fiber pulling experiments, a sized glass fiber (diameter 17 ± 1 μm) was embedded between two small pieces (ca. 10 mm in length and width) of *i*-PS films, and the obtained sandwich was then confined between two microscopy cover glasses. As described in previous papers, intense shear flow at the fiber−melt interface results from the translation of the glass fiber along its axis into the molten polymer.[18,21] This translation was performed by means of a homemade fiber pulling device, enabling one to pull the fiber at a constant linear rate, between 0 and 14 mm/s, over a distance of about 1 cm. Since the amount of fractions was very small, we have been forced to repeatedly use the same sample for different conditions. Typically, each sample was submitted to the whole thermal cycle for up to 5 or 6 times; afterward, a faint discoloring was noted and the sample was discarded.

Morphological observations during the quiescent crystallization after the application of flow were performed by a polarizing optical microscope Polyvar Pol equipped with 10× objective lens and a photo camera. Three Mettler FP 82 hot stages were used to carefully impose the thermal history described in the next paragraph.

Additional quantitative information on the lifetime of nucleation precursors were acquired by performing in situ rheooptical experiments with a Linkam CSS 450 shearing cell. To acquire direct information on the morphological features of crystals developing from oriented precursors, some scanning electron microscopy observations were also performed.

Shearing Experiments. *Fiber Pulling Experiments*. The thermomechanical protocol adopted in the fiber pulling procedure was described in detail in two preceding papers in which the lifetime of nucleation precursors in isotactic polypropylene[18] and isotactic poly(1-butene)[21] was investigated. In the present case, the ca. 300 μm thick sandwich, prepared as described above, was first held at 280 °C for 4 min to erase the memory of thermomechanical treatments imposed during the sample preparation. The sample was then quickly transferred into a Mettler FP 82 hot stage, previously set at the pulling temperature, T_P, in a range of about 20−45 °C higher than the observed melting temperature of *i*-PS (T_m = 230 °C) and above its equilibrium melting temperature ($T°_m$ = 242 °C).[50,51]

We are well aware that, being based on questionable, and indeed questioned, extrapolation procedures, evaluation of the equilibrium melting temperature of polymer crystals is rather elusive.[52,53] For isotactic polystyrene, the widely adopted value of 242 °C was obtained by the Hoffman and Weeks procedure stemming from the classical nucleation theory.[54] However, consistently with some higher measured values, a largely higher equilibrium melting temperature, T^0_m = 289 °C, was suggested by Strobl.[53] Even accepting this very high value, we remark that melt crystallization of isotactic polystyrene in quiescent conditions does not take place in the temperature range covered by our shearing experiments.

The sample was kept at T_p for 3 min, in order to reach thermal equilibrium, and then the glass fiber was pulled through the molten polymer at a rate of 5 mm/s over a distance of 5 mm. According to the equation proposed by Monasse,[45] this corresponds to a shear rate at the fiber surface around 10^3 s^{-1}. After pulling, the sample was quickly transferred into another hot stage, previously set to a suitable relaxation temperature, T_R, and there held in quiescent conditions to relax for a time, t_R. T_R can be higher, lower, or equal to T_P, but in order to avoid the development of crystallinity during relaxation, it was always kept higher than the observed melting temperature of the polymer. Finally, the sample was transferred into the third hot stage set at the isothermal crystallization temperature of 180 °C, at which the morphological observations were performed. This temperature has been chosen since it is known that isotactic polystyrene exhibits a maximum in crystal growth rate in quiescent conditions at about 180−190 °C.[55]

As described in previous papers,[18,21] a trial-and-error procedure was used to evaluate the critical holding time needed to completely erase the memory of the applied flow in the quiescent melt, t^*. In essence, a series of experiments, in which only the time elapsed between fiber pulling and quenching to T_c was changed, were performed at each T_R. In this way a morphological map was obtained from which t^* could be quantified as the mean value between the maximum holding time at T_R at which, upon cooling to T_c, transcrystallinity or high linear nucleation density is still observed around the fiber and the minimum holding time at which spherulitic morphology with uniform size is detected over the whole sample.

In Situ Rheooptical Experiments. Uniform shear field through sample thickness was conveniently applied using a Linkam CSS 450 plate−plate rotational shearing stage. To avoid morphological interferences due to development of spherulites at various depths, a gap thickness of 70 μm was always used. A step shear, at shear rate $\dot{\gamma}$ = 30 s^{-1} was imposed for a relatively short time, t_s = 10 s, at a temperature, T_s = 250 °C, higher than the melting temperature of isotactic polystyrene. The sheared sample was then cooled to 180 °C, at a cooling rate of about 30 °C/min, either immediately after the cessation of shear or after selected holding times at 250 °C. These experiments provide quantitative information in terms of nucleation density, *N*, as obtained by counting the number of pointlike nucleation centers observed in a field of known area and thickness. In these experiments anomalous results are sometimes encountered and reproducibility is rather poor;[8] however, multiple repetition of experiments, also using freshly prepared films, allows one to extract meaningful average nucleation density data. The neat

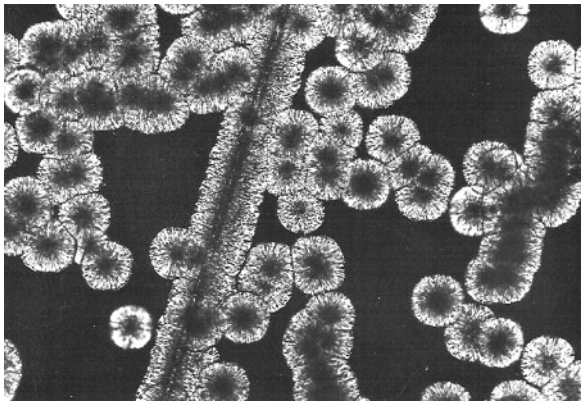

Figure 1. Transcrystalline morphology around the fiber in an unfractioned *i*-PS sample submitted to flow at 250 °C and immediately quenched to the isothermal crystallization temperature of 180 °C. Far from fiber, in the region not affected by the fiber translation, only spherulites are generated (pulling rate = 5 mm/s, pulling time = 1 s).

concentration of flow-induced nuclei, N_s, was obtained by subtracting the nucleation density measured in quiescent crystallization under the very same thermal history, N_0, from the observed nucleation density, N.

$$N_s(T_c;T_p,t_s,\dot{\gamma};T_R,t_R) = N(T_c;T_p,t_s,\dot{\gamma};T_R,t_R) - N_0(T_c) \qquad (1)$$

Morphological Observations. Some insight into the development of the semicrystalline morphology of sheared samples has been gained by SEM morphological observations. To disclose the morphological features in the early stages of the crystallization process, the noncrystallized polystyrene has been selectively dissolved using amyl acetate.[55,56] This solvent was chosen because, thanks to its mild etching action, it readily dissolves the noncrystallized material while leaving the crystalline scaffold unaltered, without further solvent-induced crystallization.[55] In order to transport away the dissolved material, drops of amyl acetate were dripped at room temperature during 30 min on the sample surface held inclined. The etched samples were then coated with a thin layer of gold and observed with a scanning electron microscope Cambridge Neo Stereoscan 440 operating at 20 kV.

Results and Discussions

Fiber Pulling Experiments. The morphology which develops in quiescent conditions after having pulled the fiber is a very sensitive marker of any residual molecular deformation associated with the flow field and surviving in the system at the instant of crystallization.[18,21] In particular, the presence of a very high nucleation density around the fiber surface, leading to the formation of cylindritic (transcrystalline) morphology, has been considered as a clear evidence of residual perturbation in the sheared polymer melt. Similar to the previously studied matrices, also in the case of i-PS the glass fiber has no intrinsic nucleating effect, as demonstrated by the uniform low nucleation density which develops after long holding times, when the polymer chains are fully relaxed. Figure 1 shows a typical example of the cylindritic morphology around the fiber that is observed when the system is quenched to 180 °C immediately after interruption of shear at 250 °C. High nucleation density is present only in a narrow region around the fiber while at some distance, where the pulled fiber had no effect on the molten polymer, only large spherulites are observed. With reference to Figure 1, we remark that since crystal growth takes place in quiescent conditions, the thickness of the transcrystalline layer nicely corresponds to the spherulitic radius, thus confirming that the growth rate does not depend on previous shear history. On the other hand, shear has a tremendous effect on nucleation

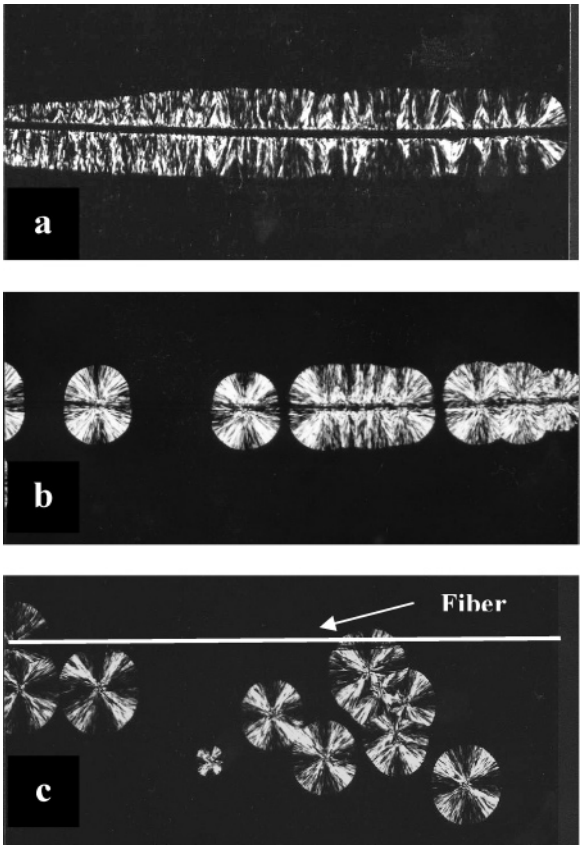

Figure 2. Morphological evolution as a function of the holding time in the melt after cessation of flow. Fraction F2 sheared and relaxed at $T_P = T_R = 260$ °C and crystallized for ca. 5 h at 180 °C: (a) $t_R = 100$ s; (b) $t_R = 300$ s; (c) $t_R = 500$ s (pulling rate = 5 mm/s, pulling time = 1 s).

density. If the sheared sample is held to relax for a short time before quenching to the crystallization temperature, the high linear nucleation density at the fiber surface is well evident (Figure 2a). On increasing the holding time, a drastic reduction in the number of crystals nucleated on the fiber surface is observed (Figure 2b). The effect of shear on the morphology is eventually fully cancelled if the relaxation is sufficiently protracted (Figure 2c).

Because of the closely spaced branches growing from the fiber surface, it is difficult to quantify the linear nucleation density by optical microscopy. Only in few fortunate conditions we were able to extract a series of rough data indicating that the concentration of shear induced nuclei exponentially decays with a single characteristic time.[48] This implies that the quasi-crystalline nanodomains produced by flow, whose existence has been proved for several polymers by SAXS experiments, are unstable entities in the superheated melt and gradually undergo destructuring if kept in quiescent conditions.[49]

To prove the progressive disappearance of shear-induced nucleation precursors, the phenomenon has also been studied at a finer spatial resolution by scanning electron microscopy. The observations were carried out on two samples sheared under the same conditions, at 250 °C, and isothermally crystallized at the same temperature, $T_c = 180$ °C. The first one was transferred to the crystallization temperature immediately after cessation of flow and left to crystallize during 15 min before the final quenching to room temperature. The second one was relaxed at 250 °C for 60 s, crystallized at 180 °C for 2 h, and then quenched. In both instances the overall crystallinity of the sample was rather low, thus favoring the selective dissolution of the amorphous parts.

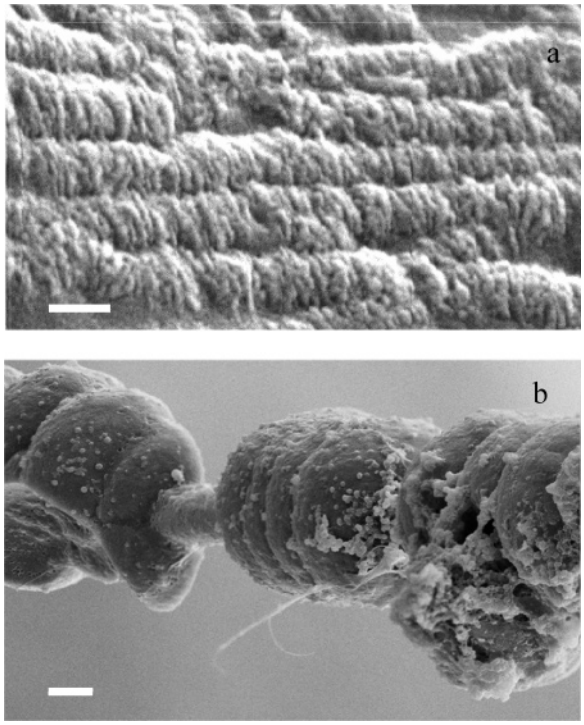

Figure 3. (a) SEM micrograph of the transcrystalline layer formed in 15 min at 180 °C in a sample quenched immediately after cessation of flow. The scale bar corresponds to 400 nm. (b) SEM micrograph of the macro-shish-kebab observed in a sample crystallized at 180 °C for 2 h after being held 1 min to relax at 250 °C. The scale bar corresponds to 20 μm. In both cases the fiber was pulled for 1 s at 5 mm/s.

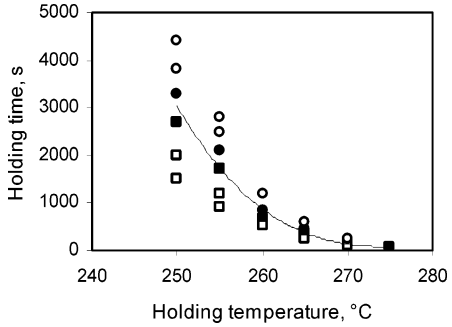

Figure 4. Morphological map of the unfractioned i-PS sample (W): (□) transcrystalline morphology or high nucleation density along the fiber surface; (○) only spherulitic morphology observed throughout the specimen. Filled symbols represent the limiting conditions at which the two types of morphologies are observed.

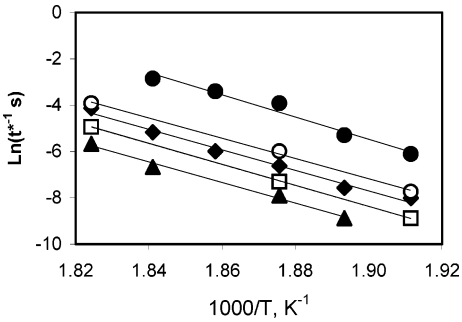

Figure 5. Temperature dependence of the relaxation rate for the i-PS fractions and the unfractioned sample. F4, M_w 1700 kg/mol (▲); F3, M_w 1022 kg/mol (□); W, M_w 939 kg/mol (◆); F2, M_w 605 kg/mol (○); F1, M_w 291 kg/mol (●).

Figure 3a shows the micrograph of the unrelaxed and briefly crystallized sample. Long stacks of lamellae, about 30 nm thick and 300−400 nm wide, which are oriented perpendicularly to the flow direction and impinge with neighbor rows, are present. This superstructure is fully consistent with the high nucleation density characteristics of transcrystalline morphology around the pulled fiber that was observed by optical microscopy. It also provides a direct evidence of the morphological picture previously inferred from the results of simultaneous micro-SAXS−WAXD experiments.[39] In this investigation it was deduced that, when shearing *i*-PS melts, bundles of few parallel chains oriented along the flow direction (shish) are first formed and then the growth of layered lamellar assemblies around 15 nm thick (kebabs) takes place, as indicated by the appearance of a very weak WAXD signal.

Figure 3b, corresponding to sample that was held 1 min to relax at 250 °C, shows a "macro-shish-kebab" morphology in which the glass fiber acts as do the shish at the molecular level. A brief relaxation is enough to dramatically reduce the nucleation density. In particular, the average distance between two developing embryonic spherulites increases from 30 nm to 20 μm. A closer examination of the fiber surface in Figure 3b does not reveal any particular morphological feature, and the glass fiber looks simply covered by a featureless polymer blanket, suggesting that no nucleation precursors has resisted the relaxation process at these locations.

From a quantitative point of view, the critical holding time, t^*, needed to attain full relaxation of the imposed mechanical perturbation and to develop a morphology indistinguishable from the one observed in quiescent conditions at the same temperature can be evaluated by the pulling fiber experiments. The acquired data are reported in Table 2. The first number corresponds to the maximum holding time at which transcrystalline morphology was observed while the second one represents the shortest holding time needed for the development of spherulites. t^* is considered to correspond to the average of these two values. As an example, the strong dependence of t^* on holding temperature after shear for the polydispersed sample is shown in the morphological map of Figure 4.

Figure 5 shows a family of parallel straight lines, shifted upward on increasing the molecular weight, that are obtained by plotting the rate of the relaxation process, as expressed by the reciprocal critical holding time, as a function of the reciprocal absolute temperature. From Figure 5 it can be appreciated that, as previously reported, the time required to recover the initial equilibrium conformation can be very long, up to many hours in the case of the high molecular weight

Table 2. Critical Holding Times, t^* (in s), for Disappearance of Transcrystalline Morphology

	M_w, × 10^{-3}				
T_R, °C	291 (F1)	605 (F2)	1022 (F3)	1700 (F4)	939 (W)
250	390−510	2000−2600	6400−7200		2700−3300
255	180−220			6000−7200	1700−2100
260	40−60	350−450	1300−1700	2500−2900	650−850
265	25−35				350−450
270	10−25			720−860	160−190
275		40−60	120−160	250−325	55−70

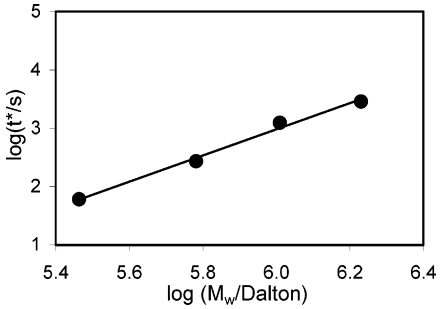

Figure 6. Dependence of the lifetime of flow-induced nucleation precursors on molecular weight at 260 °C.

sample held at relatively low temperatures (≤250 °C). The data corresponding to the unfractioned sample (M_w = 939 kg/mol) are well in line with the results obtained with sharp fractions. In facts, as shown in Figure 5, also these data can be fitted by a straight line having the same slope and lie between the straight lines corresponding to fractions with M_w = 1022 kg/mol and M_w = 605 kg/mol, respectively.

The slope of the straight lines, which represents the apparent activation energy of the rate-determining step in the process of clusters' disorientation and disorganization, is very high and substantially independent from molecular weight. Its value is around 400 kJ/mol for all samples.

The linearity of the plot log(t^*) vs log(M_w) shown in Figure 6, which corresponds to data collected at 260 °C, indicates that the characteristic time for relaxation scales according to a power law with exponent 2.2. This dependence is appreciably weaker than the one previously obtained with commercial grades of isotactic poly(1-butene) exhibiting $\bar{M}_w/\bar{M}_n > 5$, which gave a 3.4 exponent.[21] The presence of an unknown amount of high molar mass species in the commercial grade samples is likely responsible for the previously found high value of the scaling exponent. In fact, it is well-established that flow-induced crystallization is mainly dictated by the high-MW chains since only chains with molar mass higher than a critical value are involved in the formation of oriented nucleation precursors.[5,26,57] The discrepancy between the results obtained on samples with narrow and wide molecular weight distribution can be explained by considering that the value of $\bar{M}_w$ of the previously investigated poly(1-butenes) is not adequately representative of the amount of long chains which are activated in the adopted shearing conditions. The greater value of the scaling exponent indicates that the amount of chains with $M > M^*$ in the previously used polydispersed samples increases faster than $\bar{M}_w$.

In Situ Rheooptical Experiments. Quantitative information on the lifetime of shear-induced nucleation precursors have also been acquired by performing in situ rheooptical experiments in the Linkam CSS 450 cell. Shear-induced nucleation density data in unrelaxed samples and in samples held in the molten state for different times after the application of flow have been collected. The micrographs in Figure 7 illustrate the progressive decay in the nucleation density that is observed in a i-PS sample sheared at 250 °C, at a shear rate of 30 s^{-1} for 10 s, and then relaxed for 0, 60 and 180 s. As expected, the shorter is the holding time in the melt, the higher is the observed nucleation density. This series of micrographs unambiguously demonstrates that the nucleation precursors generated by the flow field are unstable entities which gradually disappear if held in quiescent conditions at the temperature at which they were formed. The reliable evaluation of nucleation density is feasible only under the "pointlike nucleation regime"; therefore, formation of row nucleated morphologies, such as those shown in Figure 7a, was avoided in the collection of data aimed at establishing the characteristics time of their relaxation.

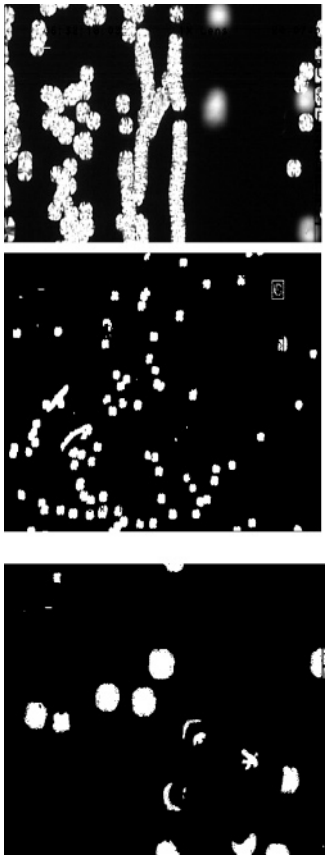

Figure 7. Morphological evidence of the decay in the number of nuclei on increasing the holding time after shear for unfractioned sample. The sample was sheared at 250 °C for 10 s at $\dot{\gamma}$ = 30 s^{-1} and held at this temperature for (a) t_R = 0 s, (b) t_R = 60 s, and (c) t_R = 180 s before isothermal crystallization at 180 °C.

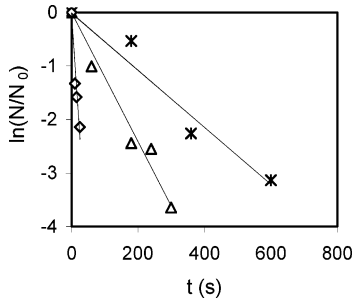

Figure 8. Fraction of surviving nucleation precursors as a function of holding time in the melt after the cessation of flow: T_R = 260 °C (◇); T_R = 250 °C (△); T_R = 240 °C (*). $T_s = T_R$; shear rate = 30 s^{-1}, shearing time = 10 s, T_c = 180 °C.

The linear trend of the data plotted in Figure 8 is consistent with the first-order decay of concentration of nucleation precursors previously conjectured:[49]

$$N = N_0 \exp\left[-\frac{t}{\tau(T)}\right] \quad (2)$$

The slope of the straight lines in Figure 8 represents the characteristics time of the process, τ. In analogy to the temperature dependence of the critical erosion time evaluated from the fiber pulling experiments previously discussed, a straight line is obtained in Figure 9 by plotting ln(τ) as a function of the reciprocal absolute temperature. In both cases, the values of the slopes, representing the apparent activation energy for

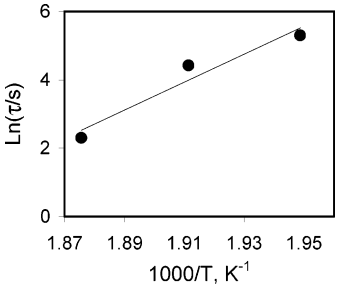

Figure 9. Temperature dependence of the characteristic time for disappearance of shear-induced nuclei.

Table 3. Parameters Used To Evaluate the Length of the Detaching Unit

sample	E_a (kJ/mol)	$\Delta H°_m$ (kJ/mol)[62]	L_u, nm[63]	L_s, nm
i-PS[a]	356	10	0.22	8.0
i-PS	400	10	0.22	8.9
i-PP[a]	260	8.7	0.22	6.5
i-PP[18]	272	8.7	0.22	6.8
POE	671	8.66	0.28	21.6
i-PBu[b 18]	732	7	0.19	20.0
i-PBu[b 21]	720	7	0.19	19.7

[a] Unpublished data. [b] Tetragonal modification.

the disappearance of flow-induced nucleation precursors, are around 300−400 kJ/mol. This suggests that the critical times, t^*, provide reliable information on the kinetics of cluster's relaxation and that, at least in the range of the shearing conditions adopted in our experiments, the rate-determining step is substantially independent from possible differences in their structural and morphological features arising from the application of flow fields of different intensity. It should be underlined that notwithstanding t^* and τ exhibiting the same temperature dependence, they are two conceptually different entities. The first one represents the time needed to recover the fully relaxed state in the melt. To attain reequilibration, each chain needs to disengage from all clusters in which it is involved. As a consequence, the critical time t^* is expected to depend on the nature of nucleation precursors, dictated by flow conditions, and on the number of precursors in which each chain is engaged, which increases with chain length. Instead, the relaxation time, τ, is an expression of the rate constant of the disorganization of each single nucleation precursor, and for this reason, it is only related to morphological features of clusters.

As reported in Table 3, very high values of the apparent activation energy were also obtained from previous fiber pulling experiments on poly(ethylene oxide), isotactic polypropylene,[18] and isotactic poly(1-butene).[21] Janeschitz-Kriegl and Eder have recently reported that relaxation phenomena in sheared polymer melts are characterized by values of the apparent activation energy similar to those obtained from our experiments.[48] To explain why the reequilibration process exhibits such a very strong temperature dependence, one can refer to the concepts put forward by Rastogi and Höhne[58−60] in their recent investigation of melting kinetics in disentangled nascent ultrahigh molecular weight polyethylene. In fact, there are analogies between the disentangled amorphous state accompanying the nascent UHMWPE and that produced by the flow field.[61] We can consider that in the unrelaxed sheared system bundles of locally aligned sequences of repeating units, forming quasi-crystalline domains, are present. Their progressive disappearance, when held in quiescent conditions, proceeds through consecutive detachment of chain stems from the outer lateral surface of the quasi crystalline nanoaggregates followed by their diffusion in the melt, thus restoring the entanglement distribution. The detaching process, which is schematized in Figure 10, represents the rate-determining step in the recover of the equilibrium coiled conformation. In the last column of Table 3, the length of the detaching stem for the polymers we have so far investigated is given. The reported stem length, L_s, corresponds to the number of detaching repeating units, which is obtained by the ratio between the apparent activation energy, E_a, and the melting enthalpy $\Delta H°_m$, multiplied by the length of the repeating unit along the *c*-axis in the corresponding crystalline lattice, L_u. For all the examined polymers, the obtained stem length ranges from 7 to 21 nm; these values are very close to that found by Rastogi et al.[58] for the melting kinetics of nascent UHMWPE. The stem lengths given in Table 3 are underevaluated because the energy needed to detach the units from the surface is certainly lower than that needed to break the interactions in the bulk of the crystal; in addition, it should be expected that the interchain interactions in the flow-induced bundles are weaker than those in an ideal crystal. In light of this consideration, the length of the detaching units, according to the suggested mechanism, is commensurate to the observed distance between the stacks of lamellae shown in Figure 3a.

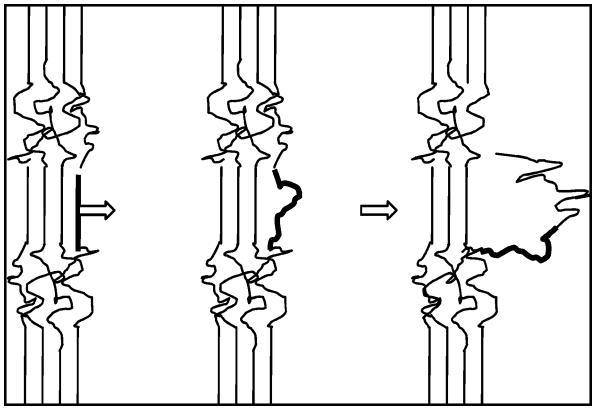

Figure 10. Schematic model for the detachment of a single stem from the surface of the oriented nucleation precursor. Once detached, the stem reptates to restore the equilibrium entanglement distribution.

This mechanism is also consistent with the recently proposed models for molecular organization in shear-induced crystal nucleation precursors,[37,64−66] and it suggests that the inner structure of row nuclei and shish is formed by a sequence of quasi-crystalline nanodomains, in which chain segments are highly oriented and well packed, alternated by regions in which a much lower level of segmental correlation exists.

Conclusions

The results obtained from fiber pulling experiments performed on a series of very narrow fractions of i-PS demonstrate that, from a phenomenological point of view, the flow-induced nucleation precursors of this polymer are long living structures alike the ones formed in isotactic poly(1-butene) and isotactic polypropylene. Thanks to the monodisperse character of the used samples, the dependence of precursors lifetime on molecular size has been better established, obtaining that the characteristic time needed to reequilibrate the sheared system scales with the molar mass according to a power law with exponent ∼2.

In situ rheooptical experiments reveal that the pointlike nucleation precursors obtained under mild shear-flow conditions relax according to an Arrhenius-like temperature dependence alike the ones which are generated at high shear rates in the fiber pulling experiments and which originate cylindritic mor-

phologies. The high apparent activation energies characterizing the process of disappearance of nucleation precursors are justified by an underlying mechanism involving, as rate-determining step, the melting and the detachment of single stems from the bundle-like domains.

Acknowledgment. This work could not have been performed without the generous offer of Prof. Hervè Marand, Virginia Tech University, who kindly donated sufficient amounts of well-characterized isotactic polystyrene fractions. The authors are grateful to the Italian Ministry of University under Project PRIN 2004-2005: "Control and Modeling of Morphology of Semi-crystalline Polymers under Realistic Processing Conditions" for partial support of this research.

References and Notes

(1) Eder, G.; Janeschitz-Kriegl, H.; Liedauer, S. *Prog. Polym. Sci.* **1990**, *15*, 629−714.
(2) Eder, G.; Janeschitz-Kriegl, H. *Mater. Sci. Technol.* **1997**, *18*, 269−342.
(3) Jay, F.; Haudin, J. M.; Monasse, B. *J. Mater. Sci.* **1999**, *34*, 2089−2102.
(4) Kumaraswamy, G.; Issaian, A. M.; Kornfield, J. A. *Macromolecules* **1999**, *32*, 7537−7547.
(5) Somani, R. H.; Hsiao, B. S; Nogales, A.; Srinivas, S.; Tsou, A. H.; Sics, I.; Baltà Calleja, F. J.; Ezquerra, T. *Macromolecules* **2000**, *33*, 9385−9394.
(6) Somani, R. H.; Hsiao, B. S.; Nogales, A.; Fruitwala, H.; Srinivas, S.; Tsou, A. H. *Macromolecules* **2001**, *34*, 5902−5909.
(7) Kumaraswamy, G.; Kornfield, J. A.; Yeh, S.; Hsiao, B. S. *Macromolecules* **2002**, *35*, 1762−1769.
(8) Koscher, E.; Fulchiron, R. *Polymer* **2002**, *43*, 6931−6942.
(9) Janeschitz-Kriegl, H.; Ratajski, E.; Steldbauer, M. *Rheol. Acta* **2003**, *42*, 355−364.
(10) Van Meerveld, J.; Peters, G. V. M.; Hutter, M. *Rheol. Acta* **2004**, *43*, 119−134.
(11) Janeschitz-Kriegl, H. *Macromolecules* **2006**, *39*, 4448−4454.
(12) Zhang, C.; Hu, H.; Wang, X.; Yao, Y.; Dong, X.; Wang, D.; Wang, Z.; Han, C. C. *Polymer* **2007**, *48*, 1105−1115.
(13) Heeley, H.; Fernyhough, C. M.; Graham, R. S.; Olmsted, P.; Inkson, N. J.; Embery, J.; Groves, D. J.; McLeish, T. C. B.; Morgovan, A. C.; Meneau, F.; Bras, W.; Ryan, A. J. *Macromolecules* **2006**, *39*, 5058−5071.
(14) Bustos, F.; Cassagnau, P.; Fulchiron, R. *J. Polym. Sci., Part B: Polym. Phys.* **2006**, *44*, 1597−1607.
(15) An, Y.; Holt, J. J.; Mitchell, G. R.; Vaughan, A. S. *Polymer* **2006**, *47*, 5643−5656.
(16) Somani, R. H.; Yang, L.; Hsiao, B. S.; Fruitwala, H. *J. Macromol. Sci., Part B: Phys.* **2003**, *42*, 515−531.
(17) Meng, K.; Zhang, X.; Zhang, C.; Han, C. *Macromol. Rapid Commun.* **2006**, *27*, 1677−1683.
(18) Alfonso, G. C.; Scardigli, P. *Macromol. Chem. Phys., Macromol. Symp.* **1997**, *118*, 323−328.
(19) Watanabe, K.; Suzuki, T.; Masabuchi, Y.; Taniguchi, T.; Takimoto, J.; Koyama, K. *Polymer* **2003**, *44*, 5843−5849.
(20) Coppola, S.; Balzano, L.; Gioffredi, E.; Maffettone, P. L.; Grizzuti, N. *Polymer* **2004**, *45*, 3249−3256.
(21) Azzurri, F.; Alfonso, G. C. *Macromolecules* **2005**, *38*, 1723−1728.
(22) Van der Beek, M. H. E.; Peters, G. W. M.; Meijer, H. E. N. *Macromolecules* **2006**, *39*, 1805−1814.
(23) Baert, J.; Van Puyvelde, P. *Polymer* **2006**, *47*, 5871−5879.
(24) Somani, R. H.; Yang, L.; Hsiao, B. S.; Sun, T.; Pogodina, N. V.; Lustiger, A. *Macromolecules* **2005**, *38*, 1244−1255.
(25) Fukushima, H.; Ogino, Y.; Matsuba, G.; Nishida, K.; Kanaya, T. *Polymer* **2005**, *46*, 1878−1885.
(26) Nogales, A.; Hsiao, B. S.; Somani, R. H.; Srinivas, S.; Tsou, A. H.; Baltà-Calleja, F. J.; Ezquerra, T. A. *Polymer* **2001**, *42*, 5247−5256.
(27) Seki, M.; Thurman, D. W.; Oberhauser, J. P.; Kornfield, J. A. *Macromolecules* **2002**, *35*, 2583−2594.
(28) Bove, L.; Nobile, M. R. *Macromol. Symp.* **2002**, *185*, 135−147.
(29) Acierno, S.; Palomba, B.; Winter, H. H.; Grizzuti, N. *Rheol. Acta* **2003**, *42*, 243−250.
(30) Elmoumni, A.; Gonzalez Ruiz, R.; Coughlin, B.; Winter, H. H. *Macromol. Chem. Phys.* **2005**, *206*, 125−134.
(31) Somani, R. H.; Yang, L.; Hsiao, B. S. *Polymer* **2006**, *47*, 5657−5668.
(32) Ogino, Y.; Fukushima, H.; Matsuba, G.; Takahashi, N.; Nishida, K.; Kanaya, T. *Polymer* **2006**, *47*, 5669−5677.
(33) Hadinata, C.; Gabriel, C.; Ruellmann, M.; Kao, N.; Laun, H. M. *Rheol. Acta* **2006**, *45*, 539−546.
(34) Eder, G.; Janeschitz-Kriegl, H.; Krobath, G. *Prog. Colloid Polym. Sci.* **1989**, *80*, 1−7.
(35) Isayev, A. I .; Chan, T. W.; Shimojo, K.; Gmerek, M. *J. Appl. Polym. Sci.* **1995**, *55*, 807−819.
(36) Chai, C. K.; Dixon, N. M.; Gerrard, D. L.; Reed, W. *Polymer* **1995**, *36*, 661−663.
(37) Somani, R. H.; Yang, L.; Hsiao, B. S.; Agarwal, P. K.; Fruitwala, H. A.; Tsou, A. H. *Macromolecules* **2002**, *35*, 9096−9104.
(38) Somani, R. H.; Yang, L.; Hsiao, B. S. *Phys. A* **2002**, *304*, 145−157.
(39) Garcia Gutierrez, M. C.; Alfonso, G. C.; Riekel, C.; Azzurri, F. *Macromolecules* **2004**, *37*, 478−485.
(40) Li, L.; De Jeu, W. H. *Macromolecules* **2003**, *36*, 4862−4867.
(41) Zuo, F.; Keum, J. K.; Yang, L.; Somani, R. H.; Hsiao, B. S. *Macromolecules* **2006**, *39*, 2209−2218.
(42) Ogino, Y.; Fukushima, H.; Takahashi, N.; Matsuba, G.; Nishida, K.; Kanaya, T. *Macromolecules* **2006**, *39*, 7617−7625.
(43) Kanaya, T.; Takayama, Y.; Ogino, Y.; Matsuba, G.; Nishida, K. In *Progress in Understanding of Polymer Crystallization, Lecture Notes in Physics;* Reiter, G., Strobl, G., Eds.; Springer: Berlin, 2007; pp 87−96.
(44) Byelov, D.; Panine, P.; De Jeu, W. H. *Macromolecules* **2007**, *40*, 288−289.
(45) Monasse, B. *J. Mater. Sci.* **1992**, *27*, 6047−6052.
(46) Janeschitz Kriegl, H. *Macromolecules* **2006**, *39*, 4448−4454.
(47) Janeschitz Kriegl, H.; Ratajsky, E. *Polymer* **2005**, *46*, 3856−3870.
(48) Janeschitz Kriegl, H.; Eder, G. *J. Macromol. Sci., Part B: Phys.* **2007**, *46*, 591−601.
(49) Ziabicki, A.; Alfonso, G. C. *Macromol. Symp.* **2002**, *185*, 211−231.
(50) Boon, J.; Challa, G.; Van Krevelen, D. W. *J. Polym. Sci., Polym. Phys. Ed.* **1968**, *6*, 1791−1801.
(51) Lemstra, P. J.; Kooistra, T.; Challa, G. J. *J. Polym. Sci., Part A-2* **1972**, *10*, 823−833.
(52) Marand, H.; Xu, J.; Srinivas, S. *Macromolecules* **1998**, *31*, 8219−8229.
(53) Al-Hussein, M; Strobl, G. *Macromolecules* **2002**, *35*, 1672−1676.
(54) Hoffman, J. D.; Weeks, J. J. *J. Res. Natl. Bur. Stand. (U.S.)* **1962**, *A66*, 13−28.
(55) Yeh, G. S.; Lambert, S. L. *J. Appl. Phys.* **1971**, *42*, 4614−4621.
(56) Padden, F. J.; Keith, H. D. *J. Appl. Phys.* **1964**, *37*, 4013−4020.
(57) Keller, A.; Kolnaar, H. W. H. *Mater. Sci. Technol.* **1997**, *18*, 189.
(58) Rastogi, S.; Lippits, D. R.; Peters, G. W .M.; Graf, R.; Yao, Y.; Spiess, H. W. *Nat. Mater.* **2005**, *4*, 635−641.
(59) Lippits, D. R.; Rastogi, S.; Höhne, G. W. H. *Phys. Rev. Lett.* **2006**, *96*, 218303.
(60) Lippits, D. R.; Rastogi, S.; Höhne, G. W. H, Mezari, B.; Magusin, P. C. M. M. *Macromolecules* **2007**, *40*, 1004−1010.
(61) Archer, L. A. *J. Rheol.* **1999**, *43*, 1617−1633.
(62) ATHAS Data Bank, http:web.utk.edu/∼athas/databank/.
(63) Alexander, L. E. In *X-ray Diffraction Methods in Polymer Science*; Burke, E., Chalmers, B., Krumhansl, J. A., Eds.; Wiley-Interscience: New York, 1969.
(64) Zhang, C.; Hu, H.; Wang, X.; Yao, Y.; Dong, X.; Wang, D.; Wang, Z.; Han, C. C. *Polymer* **2007**, *48*, 1005−1115.
(65) Somani, R. H.; Yang, L.; Sics, I.; Hsiao, B. S.; Pogodina, N. V.; Winter, H. H.; Agarwal, P.; Fruitwala, H.; Tsou, A. *Macromol. Symp.* **2002**, *185*, 105−117.
(66) Hsiao, B. S. In *Progress in Understanding of Polymer Crystallization, Lecture Notes in Physics 714*; Reiter, G., Strobl, G., Eds.; Springer: Berlin, 2007; pp 133−14.

MA071475E